Journal of Renewable Materials

Tech Science Press

DOI: 10.32604/jrm.2023.023849

check for updates

ARTICLE

Tensile Properties and Wear Resistance of Mg Alloy Containing High Si as Implant Materials

Mengqi Cong*, Yang Zhang, Yunlong Zhang, Xiao Liu, Yalin Lu and Xiaoping Li

Key Laboratory of Advanced Materials Design and Additive Manufacturing of Jiangsu Province, Jiangsu University of Technology, Changzhou, 213001, China

*Corresponding Author: Mengqi Cong. Email: congmq@jsut.edu.cn

Received: 31 July 2022 Accepted: 22 September 2022

ABSTRACT

Magnesium alloy has been considered as one of the third-generation biomaterials for the regeneration and support of functional bone tissue. As a regeneration implant material with great potential applications, in-situ Mg_2Si phase reinforced Mg-6Zn cast alloy was comprehensively studied and expected to possess excellent mechanical properties via the refining and modifying of Mg_2Si reinforcements. The present study demonstrates that the primary and eutectic Mg_2Si phase can be greatly modified by the yttrium (Y) addition. The size of the primary Mg_2Si phases can be reduced to ~20 μm with an addition of 0.5 wt.% Y. This phenomenon is mainly attributed to the poisoning effect of the Y element. Moreover, wear resistance and tensile properties of the ternary alloy have also been improved by the Y addition. Mg-6Zn-4Si-0.5Y alloy exhibits optimal tensile properties and wears resistance. The ultimate tensile strength and the elongation of the alloy with 0.5 wt.% Y are 50% and 65% higher than those of the ternary alloy, respectively. Excessive Y addition (1.0 wt.%) deteriorates the tensile properties of Mg-Zn-Si alloy. The improvement of the tensile properties is mainly due to the modification of primary and eutectic Mg_2Si phases as well as the solid solution strengthening of the Y atoms. This study provides a certain implication for the application of Mg-Zn-Si alloys containing Y elements as regeneration implants.

KEYWORDS

Magnesium alloys; Mg_2Si phase; microstructure; regeneration; mechanical properties

1 Introduction

Magnesium alloys have received widespread concern over the past decade for their potential applications in biodegradable implants because of their good biocompatibility and mechanical properties, such as guided bone regeneration (GBR) for dental implants [1–3]. In addition to its excellent biological properties, the density of Mg (1.74 g/cm^3) is very close to that of human bone (1.8–2.1 g/cm^3) [4,5]. Magnesium alloys based on the hyper-eutectic Mg-Zn-Si ternary system have great potential application in barrier membranes for GBR due to their advantages of matched bone density, excellent wear behavior, etc. [6–9]. It is well known that Mg-Zn binary system exhibits a significant age-hardening response during heat treatment [10]. Zn also plays an important role in hundreds of biological functions [11,12]. It not only promotes osteogenic activity but also inhibits the growth of many tumor cells [13,14]. Meanwhile, the appropriate addition of Si element is also beneficial to improve the tensile strength and

wear resistance of magnesium alloys, which contributes to the growth and regeneration of bone and connective tissue [15–17]. Mg_2Si phase forms after the addition of Si into magnesium alloys, which has been considered as an efficient reinforcement phase due to the superior physical properties (e.g., high melting point, high hardness and low thermal expansion coefficient [18,19]). The thermally stable Mg_2Si phase with optimal morphology and size can not only restrain the grain boundary sliding that eventually improves the mechanical properties of Mg alloys, but also greatly enhances the wear resistance.

However, the Mg_2Si phase with the morphology of coarse dendrite or Chinese script type is harmful to the mechanical behavior of magnesium alloys [20,21]. Therefore, the modification of the primary and eutectic Mg_2Si phase is of great importance to the improvement of mechanical properties for magnesium alloys. Previous studies demonstrated that the Mg_2Si phase could be modified by a variety of alloying elements, such as RE, Ca and Sb [21–25]. The addition of KBF_4 and K_2TiF_6 can also effectively influence the morphology of the Mg_2Si [26]. Among these alloying elements, RE has attracted extensive attention in the field of biomaterials due to its superior modification ability [27–29]. Jiang et al. [30] pointed out that the coarse dendritic and Chinese script type Mg_2Si crystals can be significantly refined by the addition of the Y element. However, systematic investigations on the influence of Y on the mechanical properties of in-situ synthesized high Si magnesium alloys as regeneration implants have not been reported yet. In the case of the Mg-Zn-Si system, the interactive influence of Y elements on the formation, morphology and distribution of the second phase has not been fully investigated. In addition, there will be some friction and wear of the alveolar bone under complex bite force, which may cause the implant to lose structural integrity. In order to meet the time required for bone regeneration, magnesium alloy should be able to withstand a certain external force to maintain structural integrity during the degradation of the osteogenic stage. It is necessary to have sufficient mechanical properties for Mg-base implants.

Therefore, our present work systematically studied the influence of Y addition on the microstructure, the tensile properties and the wear resistance of *in-situ* synthesized Mg_2Si/Mg-Zn alloys. The in-depth understanding of the microstructure-property relationship in this study may accelerate the potential application of magnesium alloy as regeneration implants.

2 Experimental Details

Mg-6Zn-4Si alloys were prepared by Mg (>99.9%), Zn (>99.8%) and Si ingot in an electric resistance furnace under a protective gas with 1 vol.% SF_6 + 99 vol.% Ar. The melts were kept at a temperature of 750°C for 15 min and then decanted in a preheated steel mould. Nominal amounts of Y were added into the remelted ternary alloys by means of Mg-30%Y master alloy. To meet the mechanical behavior required for bone regeneration implants, tensile properties and wear resistance were systematically studied. All samples for microstructure and tensile properties were cut from the ingots. A schematic diagram of the samples for tensile tests is shown in Fig. 1. Further details about the measurement of tensile properties are found in [31]. Considering the friction and wear in the regeneration implantation process of magnesium alloys, the wear resistance of magnesium alloy was studied under the low load of 1, 5, and 10 N. Meanwhile, the wear tests of the experimental alloys at room temperature were carried out on the friction and wear test machine (HT-500). The friction material is GCr15. A schematic diagram of the wear test is shown in Fig. 2.

Microstructure was characterized using optical microscopy (OM; XJP-300) and scanning electron microscopy (SEM; LEO 1550) affiliated with an energy dispersion spectrum (EDS). The phase formation was analyzed by X-ray diffraction system (XRD; Bruker D8-advance) employing Cu Ka radiation with a scanning rate of 1°/min and step scan of 2θ from 10° to 110°. Image-Pro Plus 6.0 was used for calculating the size of primary Mg_2Si phase.

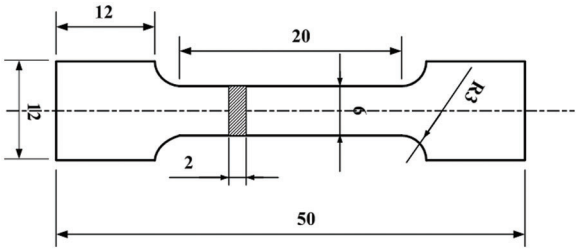

Figure 1: Schematic diagram of shape and size of the samples for tensile tests (unit: mm)

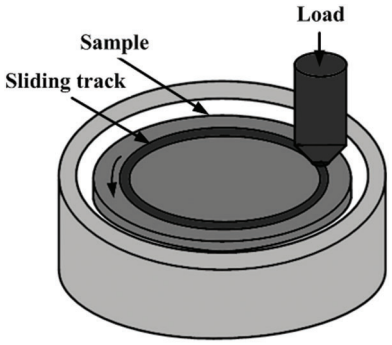

Figure 2: The schematic diagram of wear test

3 Results and Discussion

3.1 Microstructure Characterization

Fig. 3 displays the XRD patterns of as-cast Mg-6Zn-4Si alloys with different amount of Y addition. It can be seen that the main intermediate phases are Mg_2Si and MgZn in the Mg-6Zn-4Si-xY alloys. Figs. 4a–4d show the microstructural images of these alloys. As shown in Fig. 4a, the master alloy consists of α-Mg, intermetallic compound MgZn phase, primary and eutectic Mg_2Si phases (marked by red and blue circles, respectively). MgZn phase, which exhibits semicontinuous net, distributes between α-Mg and the eutectic Mg_2Si phase. The primary and eutectic Mg_2Si exist as coarse dendrites and Chinese character, respectively [31]. The size of primary Mg_2Si reaches more than 200 μm. The addition of the Y element leads to significant changes in the morphologies and distributions of the primary Mg_2Si and eutectic Mg_2Si phase as compared to the Y-free alloy. When Y content is 0.1 wt.%, the morphology of primary Mg_2Si becomes a fine polygonal structure (as shown in Fig. 4b). With increasing addition of Y up to 0.5 wt.%, all of the primary Mg_2Si phases are changed into polygonal or spherical particles, while the eutectic Mg_2Si is changed into short rods. This indicates that the refinements of both primary and eutectic Mg_2Si are very significant compared to those of lesser Y-added alloy (as shown in Fig. 4c). With a further increase in the Y content, the primary Mg_2Si becomes coarser dendritic, which is smaller in size compared to the Y-free alloy, the eutectic Mg_2Si exhibits Chinese script like morphology again. Therefore, an excessive Y addition leads to the over-modification of Mg_2Si phases, which is in conformity with the study by Jiang et al. [30]. In addition, there are some tiny granular phases in the edge of the primary Mg_2Si phase, which can be found in Fig. 4d.

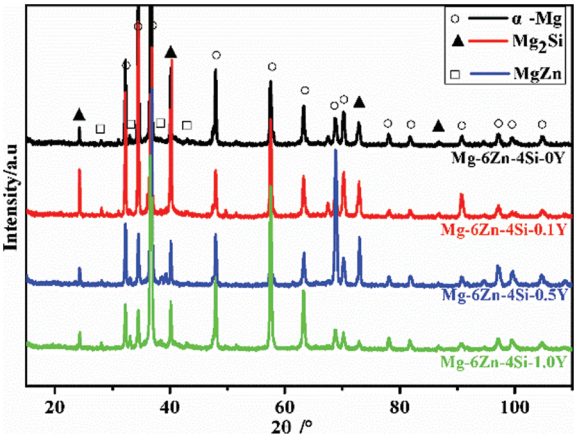

Figure 3: XRD results of the experimental alloys

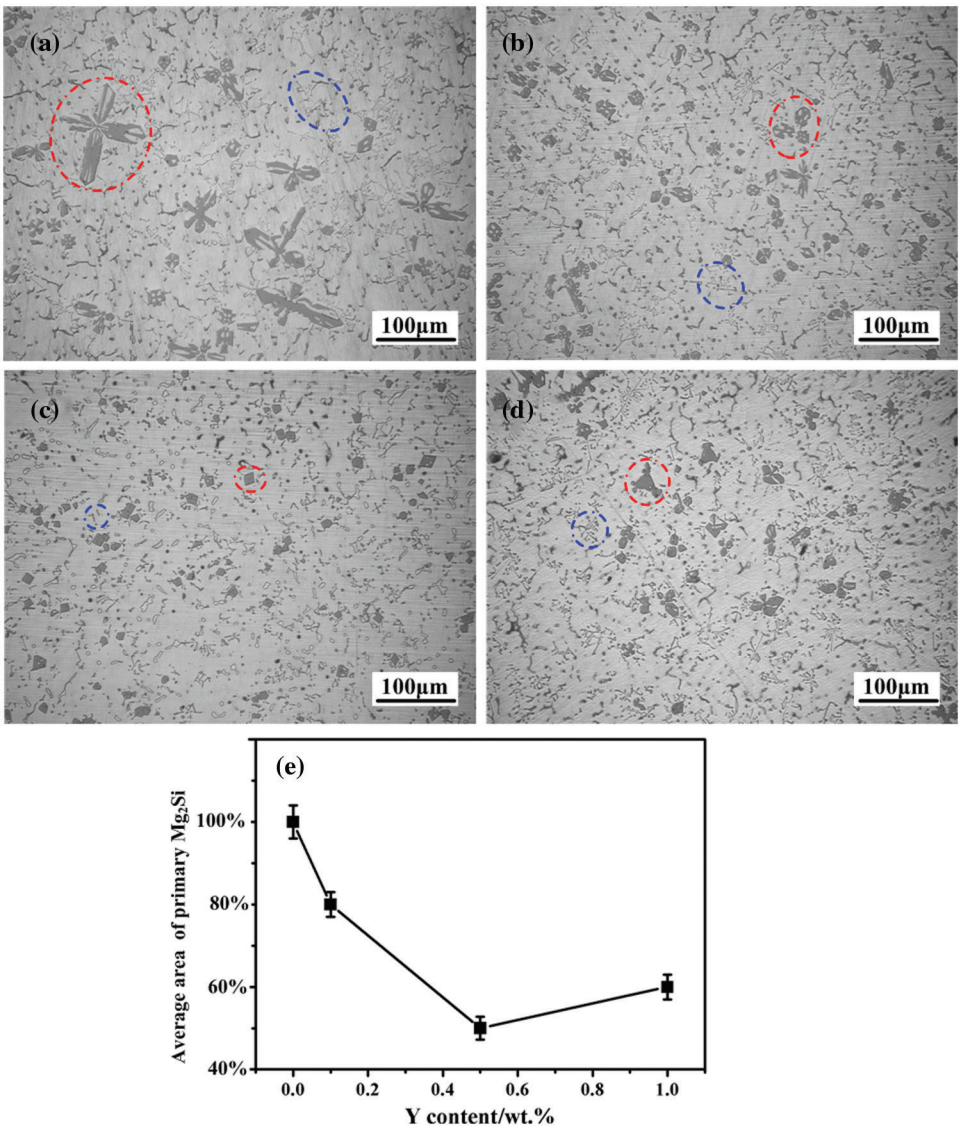

Figure 4: Optical images of the as-cast Mg-6Zn-4Si-xY alloys ((a) Without Y; (b) 0.1% Y; (c) 0.5% Y; (d) 1.0% Y) and the relationship between Y content and average area of primary Mg_2Si grains (e)

The average areas of the primary Mg_2Si phase were calculated and shown in Fig. 4e, where the average areas of the primary Mg_2Si phase in all of the alloys have been normalized with respect to that of the ternary alloy (1125.4 μm^2). It can be intuitively seen that the size of the primary Mg_2Si is significantly reduced with an addition of the Y up to 0.5 wt.%, while it goes up again with a further increase in the Y content. The smallest average area which was obtained in the Mg-6Zn-4Si-0.5Y alloy is about 478.3 μm^2 (normalized to 0.51 in Fig. 4e). The normalized results of the primary Mg_2Si phase in the alloy with 0.1 wt.% Y and 1.0 wt.% Y are 0.61 and 0.78, respectively.

The SEM image and EDS results of the tiny granular phase in the alloy with 1.0%Y are shown in Figs. 5a and 5b, respectively. As shown in Fig. 5b, the tiny granular phase consists of Mg, Si and Y atoms. In general, the possibility of compound formed among elements depends to a significant extent on the electronegativity difference. The larger the electronegativity difference, the higher the binding force among elements and thus the easier the possibility of compound formation [32]. The electronegativity differences of Mg, Si and Y atoms are displayed in Fig. 5c. The electronegativity difference between Y and Si is 0.6, while that between Y and Mg is 0, which means that Y atoms are more inclined to react with Si atoms than with Mg atoms during solidification. Combine with the EDS result, the tiny new particle in the alloy with 1.0Y addition may be Y-Si compounds. In addition, the excessive contents of Mg and Si atoms in the EDS result may be derived from Mg-Si master alloy.

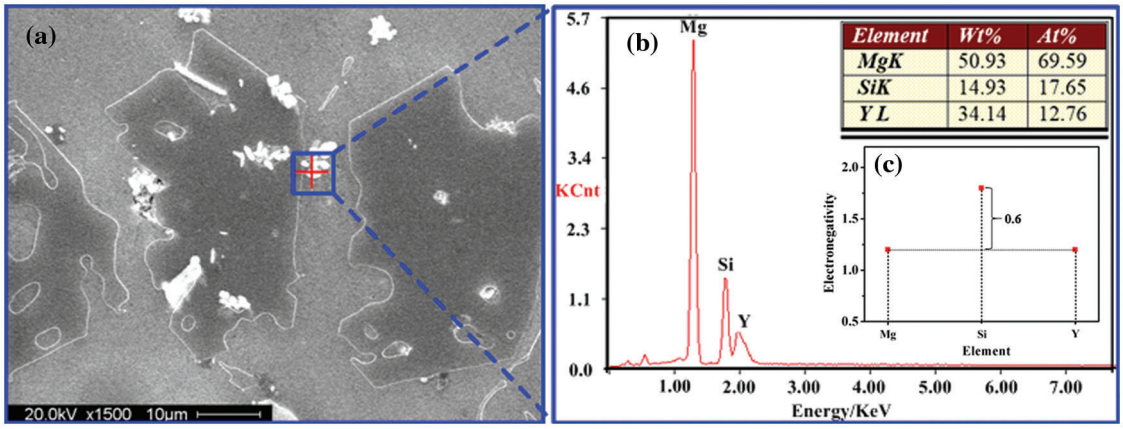

Figure 5: (a) SEM image of the as-cast Mg-6Zn-4Si-1.0Y, (b) EDS results of a tiny granular phase and (c) the electronegativity differences of Mg, Si and Y atoms

Alloying elements and refining agent can accelerate nucleation in the melt, which is a simple and effective way to modify the microstructure of Mg-base alloy [33,34]. Generally, there are two major modification and refinement mechanisms for Mg_2Si phase as stated in previous work. One is the acceleration of nucleation due to the formation of heterogeneous nucleation [35]. The other is the inhibition of crystal growth by changing the solidification condition, which is attributed to the poisoning effect [33,36]. Jiang et al. pointed out that the modification mechanism of Mg_2Si crystals modified by Y in the Mg-5Si alloy was attributed to the poisoning effect [30]. Meanwhile, the research by Lu et al. [37] indicated that the atoms of modifier element absorbed on the growth interface of silicon crystal, which leads to the impurity-induced twinning mechanism. As the atomic radius ratio of the modifier relative to Si is upon 1.65 (1.54–1.85), a growth twin will be generated at the growth interface. While the atomic radius ratio of Y ($r_Y = 2.27 \times 10^{-10}$ m) to Si ($r_{Si} = 1.46 \times 10^{-10}$ m) is 1.55. Y atoms cause lattice distortion due to their adsorption on the growth interface of the Mg_2Si crystal, which results in the

changes in crystal surface energy. Thus, the preferred growth of primary Mg_2Si crystal is suppressed by Y addition. This is also in conformity with the research by Jiang et al. [30].

As the addition of Y changes from 0.5 to 1.0 wt.%, the primary Mg_2Si phase becomes slightly coarsened, while the eutectic Mg_2Si changes to the Chinese script type again. The possible reason for this phenomenon is the consumption of Y atoms due to the formation of Y-Si compounds. Thus, the refinement and modification effect of Y on the Mg_2Si phase have been weakened, which leads to the over-modification. Therefore, it is necessary to control the Y addition at a low level. In this work, the optimum Y content is 0.5 wt.%.

3.2 Mechanical Properties

The mechanical properties of Mg-6Zn-4Si-(x)Y alloys, consisting of ultimate tensile strength (UTS) and elongation (Elong.), are displayed in Fig. 6. The ultimate tensile strength and elongation of the alloys with Y addition are higher than those of the ternary alloy, indicating that the addition of Y has dramatic benefits for the mechanical properties of the ternary alloy. The maximum of the ultimate tensile strength and elongation can be achieved for the ternary alloy with 0.5 wt.% Y addition, which are 50% and 65% higher than those of Mg-6Zn-4Si alloy, respectively. In addition, the alloy with 0.5 wt.% Y addition possesses the best mechanical properties among the Y-containing Mg-6Zn-4Si alloys. Gouveia et al. [38] and Brar et al. [39] also studied the mechanical properties of Mg-0.6Si-xZn alloys as bone implant materials and Mg-Sr(-Zn) alloys as potential biodegradable implant materials, respectively. Compared to the biodegradable magnesium alloys, the ultimate tensile strengths obtained in this study are slightly greater than Mg-Zr-Sr-Sc alloys [40], similar to Mg-4Zn-0.5Sr and Mg-0.6Si-xZn alloys with big secondary dendritic arm spacings. The elongations are slightly greater than Mg-4Zn-0.5Sr alloys, and similar to Mg-Zr-Sr-Sc alloys.

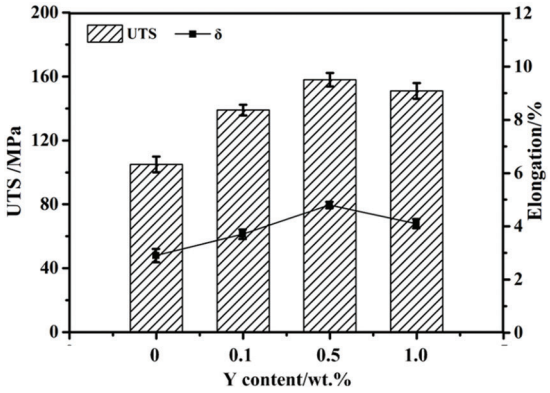

Figure 6: Mechanical properties of the experimental alloys

Fig. 7 illustrates the fracture surfaces of Mg-6Zn-4Si alloys with or without 0.5%Y. Some cleavage planes and many cracks present in the coarse primary Mg_2Si crystals can be observed in Fig. 7a. Mg_2Si crystals may lead to the intergranular failure in the ternary alloy. As the flow stress increases firstly in matrix alloy, a higher level of stress forms gradually, which will transfer to the primary Mg_2Si crystals during the tensile testing [41–43]. While the tensile stress reaches or surpasses the intrinsic fracture stress value of Mg_2Si, the crystals may fracture, which leads to the formation of cracks. Moreover, the tips of primary and eutectic Mg_2Si in ternary alloy also serve as the initiation sites of stress and crack during the tensile process, then the cracks tend to expand along the interface of α-Mg matrix and Mg_2Si phase. Thus, these cracks can link with each other and cause the fracture of Mg-6Zn-4Si alloy. The results of fracture surfaces indicate that a brittle failure type occurs in the alloy.

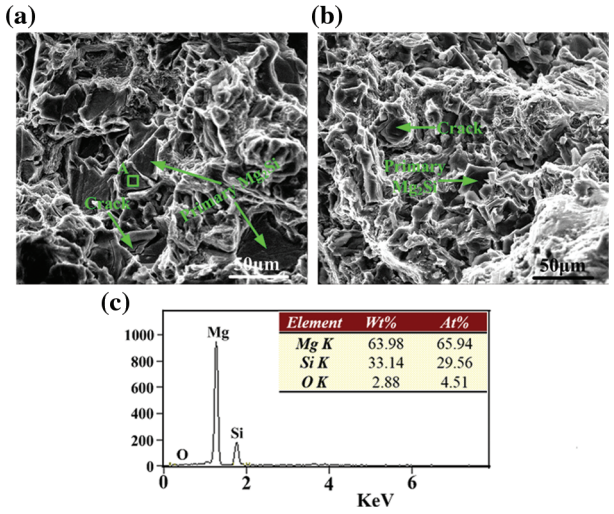

Figure 7: SEM images of the fracture surface of Mg-6Zn-4Si-xY alloys: (a) Without Y; (b) 0.5%Y; (c) EDS result of point A in Fig. 7a

Compared with Mg-6Zn-4Si alloy, less cracks and Mg_2Si crystals can be observed in Mg-6Zn-4Si-0.5Y alloy as shown in Fig. 7b. The Griffith theory pointed out that the fracture stress of composite was inversely proportional to the square root of their reinforcement phase size. Therefore, the composite with fine structure possesses high fracture stress, which is confirmed in the literature reports [44,45]. The internal defects of fine primary Mg_2Si particles are much less than those of the coarse Mg_2Si, which can significantly increase the intrinsic fracture stress value of the primary Mg_2Si crystal. As mentioned above, the addition of Y significantly changes the morphology of Mg_2Si crystals and decreases their sizes. Therefore, the mechanical properties of the ternary alloy are improved after Y addition. Besides that, the mechanical properties of engineering alloys can be effectively tailored through solution strengthening. The research by Tsuru et al. [46] has indicated that Y interacted strongly with $\frac{a}{3}\langle 11\bar{2}0\rangle$ screw dislocation, which decreased the dislocation slip anisotropy in the alloy. Its addition not only increases the stress needed for slip on the basal plane, but also enables cross-slip to prismatic and pyramidal planes, which have the potential to improve the ductility of Mg. The improvement of mechanical properties may also be attributed to the solution strengthening caused by the Y addition.

In summary, the fracture mechanism of Mg-Zn-Si alloys with Y addition is mainly attributed to the following four factors: (a) the morphological modification of the primary and eutectic Mg_2Si phases, (b) the bonding strength of α-Mg matrix and Mg_2Si phase, (c) the ease of Mg_2Si crystals crack and (d) the solid solution strengthening of Y atoms. The fracture mechanism in the present paper is almost in accordance with the research on Al-Si alloy [43], which may be due to the similarity between the Mg_2Si phase in the Mg-Si alloy and Si in the Al-Si alloy.

3.3 Wear Resistance

In the preliminary stage of guided bone regeneration for the oral cavity, a small bite force will still lead to frication and wear. Therefore, the wear test was carried out under low loads. The friction coefficient of the experimental alloys under a load of 5N is shown in Fig. 8. It can be seen that the friction coefficient of the material decreases significantly at first and then increases slowly with the increase of Y content. When the amount of Y element is 0.5 wt.%, the friction coefficient is the lowest (0.247).

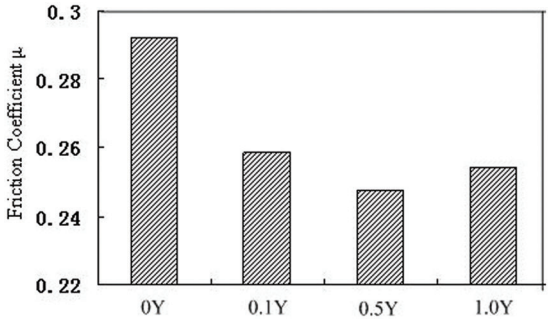

Figure 8: Friction coefficient of the experimental alloys with Y elements under a load of 5 N

Fig. 9 shows the variation curves of friction coefficient with wear time under different loads. As can be seen from the figure, the friction coefficient of the material decreases gradually with the increasing load when the wear time is consistent. With the same load, the friction coefficient increases greatly at the beginning of the friction process, finally tends to be stable gradually after dry sliding for 20 min (about 140 m), which means two stages of Mg alloys during the friction: running-in and stable period. Zhu et al. [47] studied the wear behavior of ZK60 alloy as implantation in dry environment and simulated body fluid with different PH values, they also found two stages in the dry sliding wear behavior. Literature reports [48–50] also showed that the friction between the two hard materials generated small abrasive particles, which would be carried together and gradually formed a film on the friction surface. Thus, the friction contact surface is changed from two different materials to the same material, leading to an increase in wear coefficient. In the low load, the surface temperature of magnesium alloy during dry sliding process is very low, the hardness of the friction surface keeps stable. As the load increases, the temperature of the friction interface increases, which results in the softening of the magnesium substrate on the friction surface. Therefore, the friction coefficient is small due to the reduced friction resistance of materials under high loads.

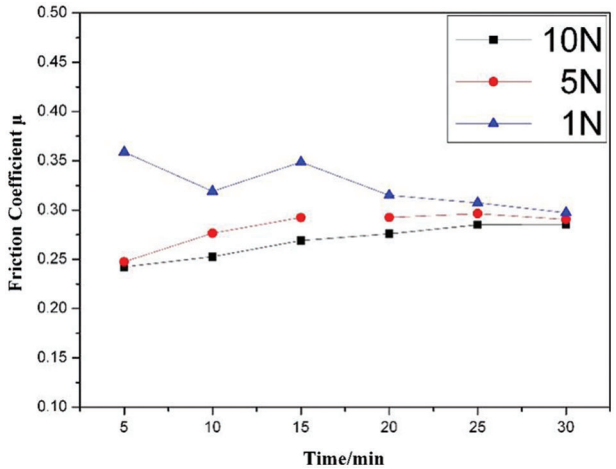

Figure 9: The relation diagram of the friction coefficient of Mg-6Zn-4Si-0.5Y alloy with the friction time under different loads

The wear rate of magnesium alloys under different loads after dry sliding for 30 min is shown in Fig. 10. The wear rate of materials increases linearly with the increasing load. The minmum of wear rate takes place in the alloy with 0.5 wt.% Y addition under low load (1 N), which is 50% less than that of Mg-6Zn-4Si alloy.

As the load is 5 or 10 N, the wear rate of Mg-6Zn-4Si alloy with 0.5 wt.% Y addition is no less than that of the base alloy. Tayebi et al. [51] also investigated wear behavior of in situ and ex situ Mg composite for implant applications, they found the similar change trend between wear rate and loads.

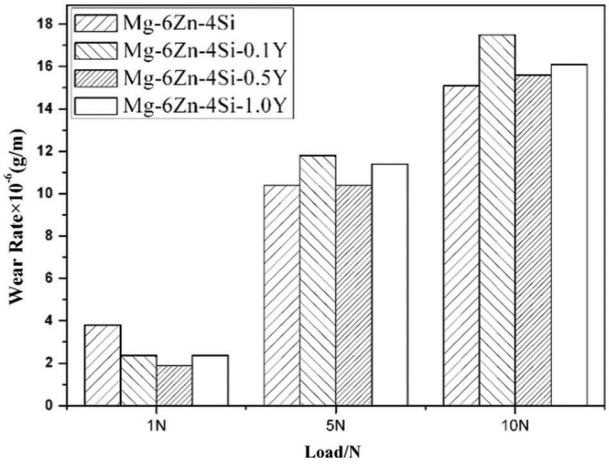

Figure 10: Wear rate of the expermental alloys under different loads after dry sliding for 30 min

Furthermore, wear behavior for the base alloy without or with 0.5 wt. % Y addition is shown in Fig. 11. It can be seen that kinds of morphologies can be obtained from the worn surfaces after wear test. Traces of parallel grooves and scallops can be observed on the surfaces of the unmodified samples (as shown in Fig. 11a). These scratches and scallops may be formed because of the detached coarse dendritic primary Mg_2Si and Chinese script-like eutectic Mg_2Si particles during the friction and wear process. The research by Mert [52] pointed out that fine microstructure could effectively improve the wear resistance of hot rolled AZ31 alloy as candidate for biodegradable implant materials. Çiçek et al. [53] also investigated the wear behavior of the Mg-Al-Si Composite, the research indicated that various parameters consisting of type, size and content of the reinforcement significantly influenced the wear behavior of the composite. In this study, the Mg_2Si phase becomes uniform by the modification of the Y element, thus the abrasion degree on the contact face between the steel ball and the experimental alloys also becomes homogeneous. In addition, the Mg_2Si phase with a small size also eases the abrasion wear. Therefore, the above factors result in the smooth surface of Mg-6Zn-4Si-0.5Y alloy (as shown in Fig. 11b).

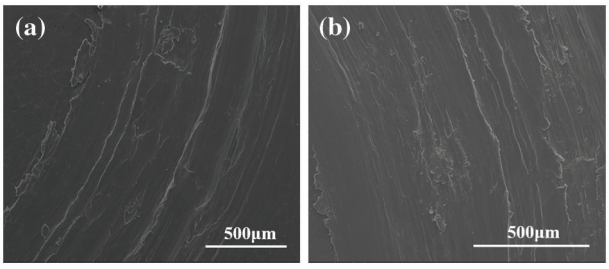

Figure 11: Characteristic scheme of worn behavior for (a) Mg-6Zn-4Si alloy, (b) Mg-6Zn-4Si-0.5Y alloy

4 Conclusions

Microstructural evolution of Mg_2Si/Mg-Zn alloy with Y addition as biomaterials, along with the mechanical properties has been systematically studied. The findings provide an optional development of

Mg-based materials as regeneration implants and enlarge the biomedical applications of Mg alloys. The conclusions are as follows:

(1) The morphologies and the size of the primary and the eutectic Mg_2Si phases can be modified by an appropriate addition of the Y element. The morphology of the primary Mg_2Si turns to fine polygons firstly and then becomes coarsened again; its size is decreased firstly and then increased with the increase of Y content. The concentrating distribution of partial Y atoms at the front zone of growing Mg_2Si crystal causes a "poisoning effect".

(2) The optimal level of Y addition effectively enhances the mechanical properties of magnesium alloys at room temperature. The alloy with 0.5 wt.% Y possesses the best ultimate tensile strength and elongation. This is mainly due to the grain refinement and the morphology optimization of the Mg_2Si particle triggered by Y addition as well solid solution strengthening of Y atoms.

(3) The appropriate addition of Y element is also beneficial for the wear resistance of the ternary alloys. The wear rate of the alloy is decreased to the lowest value at the Y content of 0.5 wt.% before a subsequent degradation with a further Y addition.

Funding Statement: This work was financially supported by Natural Science Foundation of the Jiangsu Higher Education Institutions of China (19KJD430004), the Fund of the Jiangsu CHINA-ISRAEL Industrial Technology Research Institute and Changzhou Sci & Tech Program (Nos. CJ20190042, CJ20200046).

Conflicts of Interest: The authors declare that they have no conflicts of interest to report regarding the present study.

References

1. Si, J. W., Shen, H. Z., Miao, H. W., Tian, Y., Huang, H. et al. (2021). *In vitro* and *in vivo* evaluations of Mg-Zn-Gd alloy membrane on guided bone regeneration for rabbit calvarial defect. *Journal of Magnesium and Alloys, 9(1),* 281–291. DOI 10.1016/j.jma.2020.09.013.
2. Guo, Y., Yu, Y. J., Han, L. P., Ma, S. S., Zhao, J. H. et al. (2019). Biocompatibility and osteogenic activity of guided bone regeneration membrane based on chitosan-coated magnesium alloy. *Materials Science & Engineering C, 100(S1),* 226–235. DOI 10.1016/j.msec.2019.03.006.
3. Wang, F. L., Xia, D. D., Wang, S. Y., Gu, R. L., Yang, F. et al. (2022). Photocrosslinkable Col/PCL/Mg composite membrane providing spatiotemporal maintenance and positive osteogenetic effects during guided bone regeneration. *Bioactive Materials, 13(1),* 53–63. DOI 10.1016/j.bioactmat.2021.10.019.
4. Bairagi, D., Mandal, S. (2022). A comprehensive review on biocompatible Mg-based alloys as temporary orthopaedic implants: Current status, challenges, and future prospects. *Journal of Magnesium and Alloys, 10(3),* 627–669. DOI 10.1016/j.jma.2021.09.005.
5. Xu, W. Y., Fu, P. H., Wang, N. Q., Yang, L., Peng, L. M. et al. (2022). Effects of processing parameters on fabrication defects, microstructure and mechanical properties of additive manufactured Mg-Nd-Zn-Zr alloy by selective laser melting process. *Journal of Magnesium and Alloys, 59(13),* E59. DOI 10.1016/j.jma.2022.07.005 005..
6. Chen, K., Zhao, Y., Liu, C. L., Li, Q., Bai, Y. J. et al. (2022). Novel Mg-Ca-La alloys for guided bone regeneration: Mechanical performance, stress corrosion behavior and biocompatibility. *Materials Today Communications, 32,* 103949.
7. Elyasi, M., Razaghian, A., Moharami, A., Emamy, M. (2022). Effect of Zirconium micro-addition and multi-pass friction stir processing on microstructure and tensile properties of Mg-Zn-Si alloys. *Journal of Materials Research and Technology, 20,* 4269–4282.
8. Ben-Hamu, G., Eliezer, D., Shin, K. S. (2008). The role of Mg_2Si on the corrosion behavior of wrought Mg-Zn-Mn alloy. *Intermetallics, 16(7),* 860–867.

9. Parande, G., Manakari, V., Prasadh, S., Chauhan, D., Rahate, S. et al. (2020). Strength retention, corrosion control and biocompatibility of Mg-Zn-Si/HA nanocomposites. *Journal of the Mechanical Behavior of Biomedical Materials, 103,* 103584.
10. Li, N., Wang, C., Monclús, M. A., Yang, L., Molina-Aldareguia, J. M. (2021). Solid solution and precipitation strengthening effects in basal slip, extension twinning and pyramidal slip in Mg-Zn alloy. *Acta Materialia, 221,* 117374.
11. Wu, Y., He, G., Zhang, Y., Liu, Y., Li, M. et al. (2016). Unique antitumor property of the Mg-Ca-Sr alloys with addition of Zn. *Scientific Reports, 6(1),* 21736. DOI 10.1038/srep21736.
12. Zhou, H., Liang, B., Jiang, H. T., Deng, Z. L., Yu, K. X. (2021). Magnesium-based biomaterials as emerging agents for bone repair and regeneration: From mechanism to application. *Journal of Magnesium and Alloys, 9(3),* 779–804. DOI 10.1016/j.jma.2021.03.004.
13. Meng, X., Jiang, Z. T., Zhu, S. J., Guan, S. K. (2020). Effects of Sr addition on microstructure, mechanical and corrosion properties of biodegradable Mg-Zn-Ca alloy. *Journal of Alloys and Compounds, 838,* 155611. DOI 10.1016/j.jallcom.2020.155611.
14. Puvvada, N., Rajput, S., Kumar, B. N. P., Sarkar, S., Konar, S. et al. (2015). Novel ZnO hollow-nanocarriers containing paclitaxel targeting folate-receptors in a malignant pH-microenvironment for effective monitoring and promoting breast tumor regression. *Scientific Reports, 5(1),* 11760. DOI 10.1038/srep11760.
15. Yuan, G. Y., Liu, M. P., Ding, W. J., Inoue, A. (2003). Microstructure and mechanical properties of Mg-Zn-Si-based alloys. *Materials Science & Engineering A, 357(1–2),* 314–320. DOI 10.1016/S0921-5093(03)00208-9.
16. Zhang, E. L., Yang, L., Xu, J. W., Chen, H. Y. (2010). Microstructure, mechanical properties and bio-corrosion properties of Mg-Si(-Ca, Zn) alloy for biomedical application. *Acta Biomaterialia, 6(5),* 1756–1762.
17. Gil-Santos, A., Marco, I., Moelans, N., Hort, N., Biest, O. V. D. (2017). Microstructure and degradation performance of biodegradable Mg-Si-Sr implant alloys. *Materials Science and Engineering C, 71,* 25–34.
18. Zhou, X., Guo, T., Wu, S., Lv, S. L., Yang, X. et al. (2018). Effects of Si content and Ca addition on thermal conductivity of as-cast Mg-Si alloys. *Materials, 11(12),* 2376.
19. Dong, H., Xiang, S. M., Lv, J., Wang, Y., Li, L. et al. (2020). Modification of Mg_2Si phase morphology in Mg-4Si alloy by Sb and Nd additions. *Journal of Materials Engineering and Performance, 29,* 3678–3687.
20. Moussa, M. E., Waly, M. A., El-Sheikh, A. M. (2014). Effect of Ca addition on modification of primary Mg_2Si, hardness and wear behavior in Mg-Si hypereutectic alloys. *Journal of Magnesium and Alloys, 2(3),* 230–238.
21. Xiao, P., Gao, Y. M., Mao, P., Yang, C. C., Tun, K. S. et al. (2021). Revealing modification mechanism of Mg_2Si in Sb modified Mg_2Si/AZ91 composites and its effect on mechanical properties. *Journal of Alloys and Compounds, 850,* 156877.
22. Guo, T., Wu, S. S., Zhong, X., Lv, S. L., Xia, L. Q. (2020). Effects of Si content and Ca modification on microstructure and thermal expansion property of Mg-Si alloys. *Materials Chemistry and Physics, 253,* 123260.
23. Lotfpour, M., Emamy, M., Dehghanian, C., Poubahari, B. (2018). Ca addition effects on the microstructure, tensile and corrosion properties of Mg matrix alloy containing 8 wt.% Mg_2Si. *Journal of Materials Engineering and Performance, 27,* 411–422.
24. Hu, B., Zhu, W. J., Li, Z. X., Lee, S. B., Li, D. J. et al. (2021). Effects of Ce content on the modification of Mg_2Si phase in Mg-5Al-2Si alloy. *Journal of Magnesium and Alloys*. DOI 10.1016/j.jma.2021.08.031.
25. Han, W. D., Li, K., Hu, F., Li, Y. H., Tang, B. B. (2019). Microstructure and mechanical properties of Mg-2.5Si-xCe in-situ particle reinforced composites prepared by rapid solidification process. *Results in Physics, 15,* 102509.
26. Wang, H. Y., Jiang, Q. C., Ma, B. X., Wang, Y., Wang, J. G. et al. (2005). Modification of Mg_2Si in Mg-Si alloys with K_2TiF_6, KBF_4 and KBF_4 + K_2TiF_6. *Journal of Alloys and Compounds, 387(1–2),* 105–108.
27. Zhu, T. L., Cui, C. L., Zhang, T. L., Wu, R. Z., Betsofen, S. et al. (2014). Influence of the combined addition of Y and Nd on the microstructure and mechanical properties of Mg-Li alloy. *Materials & Design, 57,* 245–249.
28. Weng, W. J., Biesiekierski, A., Li, Y. C., Dargusch, M., Wen, C. (2021). A review of the physiological impact of rare earth elements and their uses in biomedical Mg alloys. *Acta Biomaterialia, 130,* 80–97.

29. Yang, L. Z., Feng, Y., He, Y. Q., Yang, L. Y., Liu, H. C. et al. (2022). Effect of Sc/Sm microalloying on microstructural and properties of Mg-2Zn-0.3Ca biodegradable alloy. *Journal of Alloys and Compounds, 907,* 164533.
30. Jiang, Q. C., Wang, H. Y., Wang, Y., Ma, B. X., Wang, J. G. (2005). Modification of Mg_2Si in Mg-Si alloys with yttrium. *Materials Science & Engineering A, 392(1–2),* 130–135.
31. Cong, M. Q., Li, Z. Q., Liu, J. S., Li, S. H. (2014). Effect of Sr on microstructure, tensile properties and wear behavior of as-cast Mg-6Zn-4Si alloy. *Materials & Design, 53,* 430–434.
32. Ye, L. Y., Hu, J. L., Tang, C. P., Zhang, X. M., Deng, Y. L. et al. (2013). Modification of Mg_2Si in Mg-Si alloys with gadolinium. *Materials Characterization, 79,* 1–6.
33. Shin, H. C., Son, J., Min, B. K., Choi, Y. S., Cho, K. M. et al. (2019). The effect of Ce on the modification of Mg_2Si phases of as-cast eutectic Mg-Si alloys. *Journal of Alloys and Compounds, 792,* 59–68.
34. Lotfpour, M., Bahmani, A., Mirzadeh, H., Emamy, M., Malekan, M. et al. (2021). Effect of microalloying by Ca on the microstructure and mechanical properties of as-cast and wrought Mg-Mg_2Si composites. *Materials Science & Engineering A, 820,* 141574.
35. Sun, J. Y., Li, C., Liu, X. F., Yu, L. M., Li, H. J. et al. (2018). Investigation on AlP as the heterogeneous nucleus of Mg_2Si in Al-Mg_2Si alloys by experimental observation and first-principles calculation. *Results in Physics, 8,* 146–152.
36. Wang, H. Y., Zheng, N., Wang, W., Gu, Z. H., Li, D. et al. (2008). Modification of Mg_2Si in Mg-4Si alloys with B. *ISIJ International, 48(11),* 1662–1664.
37. Lu, S. Z., Hellawell, A. (1987). The mechanism of silicon modification in aluminum-silicon alloys: Impurity induced twinning. *Metallurgical and Materials Transactions A, 18,* 1721–1733.
38. Gouveia, G. L., Garcia, A., Spinelli, J. E. (2021). Towards a morphological control of Mg_2Si and superior tensile properties of high-Zn Mg-0.6Si (-Zn) alloys. *Materials Letters, 299,* 130084.
39. Brar, H. S., Wong, J., Manuel, M. V. (2012). Investigation of the mechanical and degradation properties of Mg-Sr and Mg-Zn-Sr alloys for use as potential biodegradable implant materials. *Journal of the Mechanical Behavior of Biomedical Materials, 7,* 87–95.
40. Munir, K., Lin, J. X., Wen, C., Wright, P. F. A., Li, Y. C. (2020). Mechanical, corrosion, and biocompatibility properties of Mg-Zr-Sr-Sc alloys for biodegradable implant applications. *Acta Biomaterialia, 102,* 493–507.
41. Hu, T., Wang, F., Zheng, R. X., Xiao, W. L., Li, Y. et al. (2019). Effects of B and Sn additions on the microstructure and mechanical property of Mg-3Al-1Si alloy. *Journal of Alloys and Compounds, 796,* 1–8.
42. Xu, C. L., Wang, H. Y., Yang, Y. F., Jiang, Q. C. (2007). Effect of Al-P-Ti-TiC-Nd_2O_3 modifier on the microstructure and mechanical properties of hypereutectic Al-20 wt.%Si alloy. *Materials Science & Engineering A, 452–453,* 341–346.
43. Li, Q. L., Xia, T. D., Lan, Y. F., Li, P. F., Fan, L. (2013). Effects of rare earth Er addition on microstructure and mechanical properties of hypereutectic Al-20%Si alloy. *Materials Science & Engineering A, 588,* 97–102.
44. Cong, M. Q., Li, Z. Q., Liu, J. S., Yan, M. Y., Chen, K. et al. (2012). Effect of Ca on the microstructure and tensile properties of Mg-Zn-Si alloys at ambient and elevated temperature. *Journal of Alloys and Compounds, 539,* 168–173.
45. Azarbarmas, M., Emamy, M., Rassizadehghani, J., Alipour, M., karamouz, M. (2011). The influence of beryllium addition on the microstructure and mechanical properties of Al-15%Mg_2Si in-situ metal matrix composite. *Materials Science & Engineering A, 528(28),* 8205–8211.
46. Tsuru, T., Chrzan, D. (2015). Effect of solute atoms on dislocation motion in Mg: An electronic structure perspective. *Scientific Reports, 5,* 8793.
47. Zhu, T., Yu, Y., Shen, Y. S., Xiong, Y. (2021). Wear behavior of extruded ZK60 magnesium alloy in simulated body fluid with different pH values. *Materials Chemistry and Physics, 262,* 124292.
48. Asl, K. M., Masoudi, A., Khomamizadeh, F. (2010). The effect of different rare earth elements content on microstructure, mechanical and wear behavior of Mg-Al-Zn alloy. *Materials Science and Engineering A, 527(7–8),* 2027–2035.
49. Das, S., Morales, A. T., Alpas, A. T. (2010). Microstructural evolution during high temperature sliding wear of Mg-3% Al-1% Zn (AZ31) alloy. *Wear, 268(1–2),* 94–103.

50. Zhang, Y. B., Yu, S. R., Luo, Y. R., Hu, H. X. (2008). Friction and wear behavior of as-cast Mg-Zn-Y quasicrystal materials. *Materials Science and Engineering A, 472(1–2),* 59–65.
51. Tayebi, M., Bizari, D., Hassanzade, Z. (2020). Investigation of mechanical properties and biocorrosion behavior of in situ and ex situ Mg composite for orthopedic implants. *Materials Science and Engineering, 113,* 110974.
52. Mert, F. (2017). Wear behaviour of hot rolled AZ31B magnesium alloy as candidate for biodegradable implant material. *Transactions of Nonferrous Metals Society of China, 27(12),* 2598–2606.
53. Çiçek, B., Ahlatç, H., Sun, Y. (2013). Wear behaviours of Pb dded Mg-Al-Si composites reinforced with *in-situ* Mg_2Si particles. *Materials & Design, 50,* 929–935.